American Mineralogist, Volume 77, pages 462–473, 1992

High-pressure ^{57}Fe γ resonance and compressibility of $Ca(Fe,Mg)Si_2O_6$ clinopyroxenes

LI ZHANG,* STEFAN S. HAFNER
Institute of Mineralogy, University of Marburg, 3550 Marburg, Germany

ABSTRACT

Three synthetic samples of the hedenbergite-diopside join $Ca(Fe_xMg_{1-x})Si_2O_6$ ($x = 1$, $x = 0.80$, and $x = 0.60$) were studied between ambient conditions and 10 GPa (293 K) by use of ^{57}Fe γ resonance (Mössbauer effect) with a clamp-technique pressure cell. The isomer shift δ and quadrupole splitting ΔE_Q of Fe^{2+} at the M1 position decrease with increasing pressure. They exhibit a discontinuity between 3.8 and 4.3 GPa in all three samples, indicating a reversible phase transition of first order. An approximately linear relationship between δ and ΔE_Q was observed. The value of δ at constant pressure is independent of Fe/Mg ratio, whereas ΔE_Q decreases with decreasing Fe/Mg ratio. The $\partial\delta/\partial \ln V$ and $\partial\Delta E_Q/\partial \ln V$ values were derived.

The axial and volume compressibilities of two samples ($x = 1$ and $x = 0.60$) were determined from the unit-cell parameters measured by powder X-ray diffraction between ambient pressure and 10 GPa using a diamond-anvil cell. The axial compressibility ratio $\beta_a:\beta_b:\beta_c$ of hedenbergite is 0.65(4):1.00(6):0.79(6). Isothermal bulk moduli for Hd and $Hd_{60}Di_{40}$ were determined by fitting a Birch-Murnaghan equation of state to the pressure-volume data, assuming $K_0' = 4$. They are 119(2) and 82.7(1) GPa, respectively. An inverse relationship of the unit-cell parameters between pressure and temperature was observed.

Pressure change in δ below 4 GPa results mainly from changes in Fe^{2+} valence orbitals. The change in ΔE_Q is due to changes in the three lowest 3d orbitals of Fe^{2+} coupled with changes in octahedral geometry. For the changes in δ and ΔE_Q above 4 GPa, changes in overlap between Fe^{2+} and ligand orbitals are important.

The decrease in ΔE_Q with decreasing Fe/Mg ratio at constant pressure results mainly from the change in geometry of the M1 octahedra occupied by Fe^{2+}. The relatively invariable δ in the three samples at constant pressure suggests that the bond distances of the Fe^{2+} octahedra are distinct from those of the Mg^{2+} octahedra.

INTRODUCTION

Pyroxenes with compositions near $Ca(Fe,Mg)Si_2O_6$ have drawn attention over more than half a century mainly because of their important role in the Earth's lower crust and upper mantle. The end-members diopside $CaMgSi_2O_6$ and hedenbergite $CaFeSi_2O_6$ have been the subject of many experimental studies. Whereas the crystal structures and physical properties of the $Ca(Fe,Mg)Si_2O_6$ system are well known at ambient conditions, there are comparatively few crystallographic data obtained simultaneously at high temperatures and high pressures that correspond to the conditions of the lower crust or upper mantle. However, experimental studies carried out either at high temperature or high pressure have been reported on isothermal compression (Vaidya et al., 1973), thermal expansion (Cameron et al., 1973), elasticity (Levien et al., 1979; Kandelin and Weidner, 1988), temperature or pressure effects on the crystal structure (Cameron et al., 1973; Levien and Prewitt, 1981), phase transformations at high pressure or high temperature (Kim et al., 1989; Tamai and Yagi, 1989), and so forth.

Although some compositions of the system $Ca(Fe,Mg)Si_2O_6$ have been examined extensively at high temperatures, data from high-pressure experiments are more limited. Important problems concerning the nature of atomic bonding at high pressure, its initiating role in phase transitions, and its effect on some of the physical properties are still open to question. Progress in this direction requires more accurate data on details of the atomic bond as a function of temperature and pressure within the temperature-pressure stability field of pyroxene.

High-pressure ^{57}Fe γ resonance (Mössbauer effect) may provide detailed information on the pressure-dependent behavior of Fe at its crystallographic site, its bonding to the adjacent ligands, polyhedral distortion, etc. Since such measurements probe directly the properties of the crystallographic site in question, they are sensitive to electronic properties at the site and to subtle local changes depending on pressure or temperature. They may be complementary to structural refinements by diffraction techniques.

* Present address: Max-Planck-Institut für Chemie, Postfach 3060, W6500 Mainz, Germany.

0003–004X/92/0506–0462$02.00

The Mössbauer effect of ^{57}Fe at high pressure has been hampered in the past for three reasons: (1) the high-pressure technique adapted (Stanek et al., 1986a) was limited to a pressure range that was low compared with the rather small compressibility of the relevant mineral, (2) pressure calibration was not continuous over the entire range of pressure applied, and (3) the absorber was thick compared with the resolution required and consequently the resonant absorption curves were deformed (Burns et al., 1972; Huggins et al., 1974). To overcome these difficulties, new techniques were employed in the present study.

The aims of the present work on the $Ca(Fe,Mg)Si_2O_6$ system were, first, to observe the effect of pressure on the electronic structure of Fe^{2+}; second, to correlate the ^{57}Fe hyperfine data with those of the unit cell at high pressure; and third, to study the dependence of the Fe^{2+} electronic structure on chemical composition at high pressures.

Experimental

Samples

Clinopyroxene samples with compositions along the hedenbergite-diopside join with Fe/(Fe + Mg) ratios according to Hd, $Hd_{80}Di_{20}$, and $Hd_{60}Di_{40}$ were synthesized hydrothermally at 600 °C and 0.1 GPa H_2O vapor pressure over a period of 7 d. Ferrous oxalate (natural abundance of ^{57}Fe) was used for the synthesis. The products were examined with X-ray diffraction as well as ^{57}Fe γ resonance at ambient conditions. No foreign phases were detected. The experimental products were finely ground for the ^{57}Fe experiments. The samples Hd and $Hd_{60}Di_{40}$ were also studied using powder X-ray diffraction at high pressure for determination of the linear and volume compressibilities (Zhang et al., 1989).

Mössbauer effect of ^{57}Fe at high pressures

The high-pressure ^{57}Fe resonance experiment was carried out by use of the clamp technique. The pressure cell consists of two symmetric Bridgman-type B_4C anvils (Moser et al., 1980). Each anvil was bound and supported by two rings made of hardened $Cu_{0.98}Be_{0.02}$ (CuBe). The assembly as shown in Figure 1 was placed in a CuBe clamp. Pressure was established by a hydraulic press and maintained by tightening the clamp, which was removed subsequently from the press for the ^{57}Fe experiment. The sample was contained in the pyrophyllite gasket. An external steel ring outside the pyrophyllite gasket kept variation of the sample area to a minimum. Paraffin (melting point 45–50 °C) was used as the pressure-transmitting medium.

The relatively large sample volume (about 3.5 mm^3) of the high-pressure cell makes it possible to place manometers of metallic Pb and Bi into the cell (cf. Fig. 1). This permits continuous, in situ calibration of the pressure by measuring the electrical resistance of Pb and observing the abrupt change of Bi electrical resistance at the three phase-transition points 2.55, 2.69, and 7.3 GPa (Eiling and Schilling, 1981). Simultaneous use of the two pressure calibrants enabled continuous determination of pressure between 0 and 13 GPa. The error of the pressure determination was estimated to be ±0.1–0.5 GPa, yielding a larger error at higher pressure. An estimate of the pressure gradient was also possible from the observation of the sharpness of the Bi phase transitions. The observed pressure gradients depended on the absolute value of pressure. In our experiments, they were 2–3% at 2.55 GPa and 5–7% at 7.3 GPa.

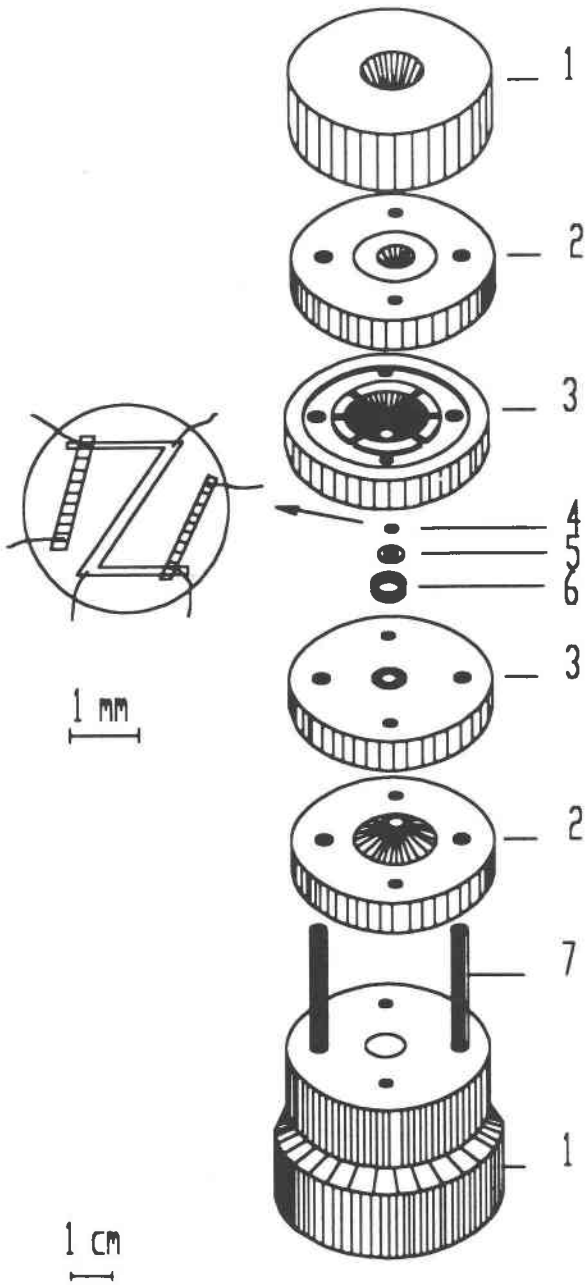

Fig. 1. High-pressure cell assembly: 1, backing ring (CuBe); 2, binding ring (CuBe); 3, supporting ring (CuBe) for B_4C anvil; 4, pressure manometer, shaded strips are metallic Bi, open strip is metallic Pb; 5, gasket (pyrophyllite); 6, ring (steel); scales are approximate.

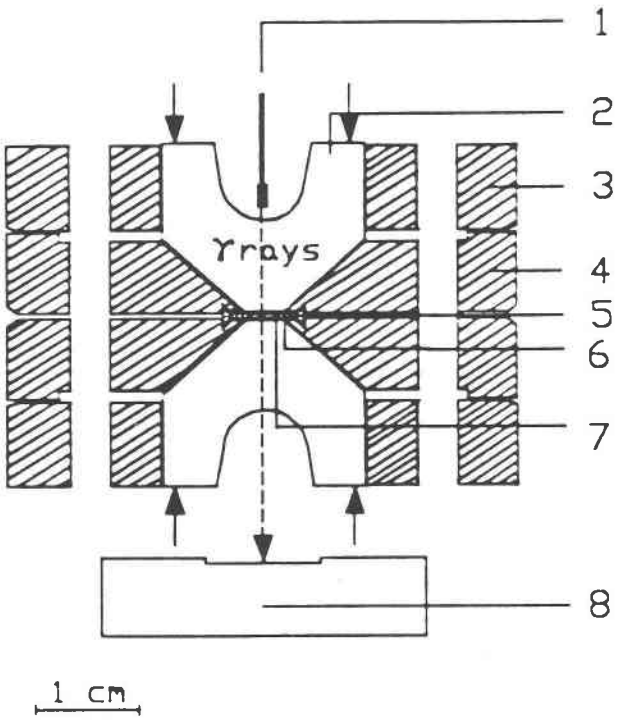

Fig. 2. Cross section of the high-pressure cell: 1, ^{57}Co point source; 2, upper B_4C anvil; 3, binding ring; 4, supporting ring; 5, ring; 6, gasket; 7, absorber; 8, detector (proportional counter).

One of the advantages of using B_4C anvils is the relatively large area of the anvil face available for resonant absorption (0.13 cm^2). This allows the use of thin absorbers. Absorber thickness in Fe was about 5 mg/cm^2 (0.11 mg ^{57}Fe/cm^2 based on natural concentration). It was not necessary to use samples enriched in ^{57}Fe for this study.

The ^{57}Fe spectra at high pressures were recorded using a transmission setup as shown in Figure 2. We used ^{57}Co/Rh point sources of 10–25 mCi. The ratio R/d was about 0.21, the line broadening resulting from the "cosine smearing effect" (Spijkerman et al., 1965) being reasonably small. Here R is the radius of detector window and d, the distance between source and detector.

Two mirror-symmetrical spectra were recorded simultaneously in a 1024 channel analyzer using constant acceleration. The total number of counts for a spectrum was about 10^6 per channel. The spectra were fitted after folding to 512 channels. The point of zero velocity was obtained by the least-squares method in the folding procedure. Recording a spectrum generally required 4–7 d depending on the strength of the source. Source and absorber were held at 293 K over the period of experiment. In view of the rather small pressure-induced changes in the ^{57}Fe hyperfine parameters of the $Ca(Fe,Mg)Si_2O_6$ system, we attempted to attain identical conditions with respect to such factors as geometry, counting rate, γ-ray scattering, and Doppler velocity control for the recording of each spectrum.

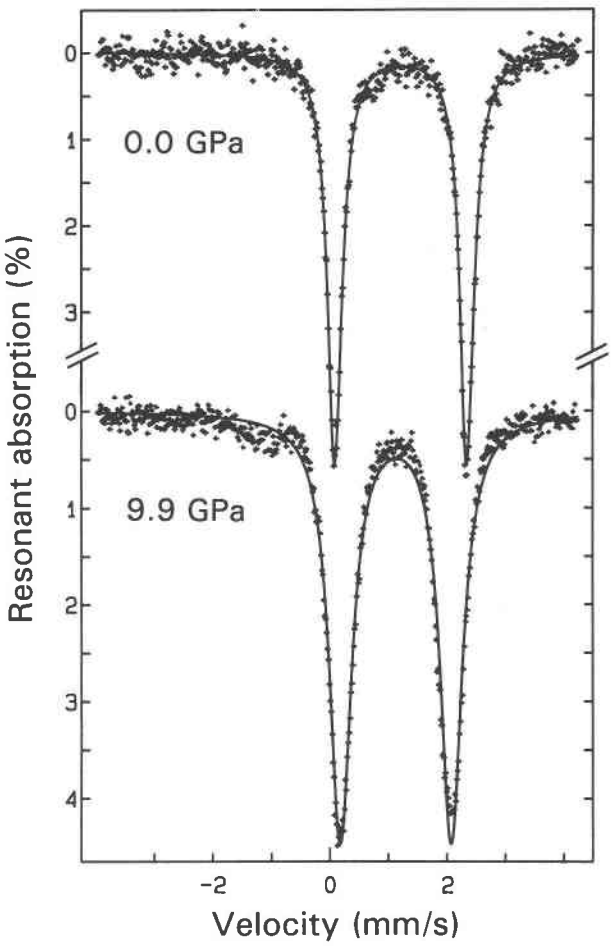

Fig. 3. Spectra for ^{57}Fe of synthetic hedenbergite at ambient conditions and 9.9 GPa (293 K); the doublet is due to Fe^{2+} at M1.

In general, B_4C used for the anvils contains small traces of Fe, which yield a rather complex ^{57}Fe spectrum with paramagnetic, superparamagnetic, and magnetic components arising from chemically not-well-defined Fe-containing particles. This ^{57}Fe spectrum was the same at ambient pressure and at 10 GPa. The intensity of the strongest line in this spectrum was about 2%. Since it is important to keep the absorbers reasonably thin, it was necessary to determine this superimposed background spectrum for each pair of anvils by a precursor experiment without pyroxene absorber using the same total count number as for the sample spectrum. The pyroxene spectra were corrected by deduction of the (raw) background spectrum from the sample spectrum using a least-squares fitting procedure. The resulting resonant absorption of the pyroxene lines was 3–4%. The background correction because of Fe contamination of the anvils produced by far the largest contribution to the total error of the determined hyperfine parameters.

The intensities and widths of the two lines of the observed ^{57}Fe doublet at ambient conditions were equal

TABLE 1. Values of ^{57}Fe hyperfine parameters at M1 in Hd between 0 and 10 GPa (293 K)

Pressure (GPa)	δ* (mm/s)	ΔE_Q (mm/s)	Γ** (mm/s)	χ^2
0.0†	1.198(1)	2.253(2)	0.304(3)	0.85
0.8	1.189(1)	2.233(2)	0.294(4)	0.51
1.5	1.179(1)	2.217(2)	0.314(3)	0.57
1.9	1.175(1)	2.197(2)	0.324(2)	0.70
2.6	1.178(1)	2.182(2)	0.328(3)	1.16
3.2	1.172(1)	2.165(2)	0.330(3)	0.71
4.2	1.160(1)	2.131(2)	0.360(3)	0.74
4.4	1.145(2)	2.026(3)	0.386(5)	2.53
5.7	1.142(2)	1.993(3)	0.440(5)	0.83
7.9	1.131(1)	1.971(2)	0.418(4)	1.28
9.2	1.129(1)	1.886(3)	0.460(5)	1.73
9.9	1.121(1)	1.894(3)	0.460(5)	1.86

Note: Standard deviations are given in parentheses. Experiments at 5.7, 9.2, 3.2, 0.0 GPa; at 1.9, 4.2, 7.9, 9.9 GPa; and at 1.5, 0.8 GPa were consecutive experiments.

* Referred to metallic Fe at ambient conditions.

** Full width at half intensity.

† Measured after the experiment at 9.2 GPa.

TABLE 2. Values of ^{57}Fe hyperfine parameters at M1 in $Hd_{80}Di_{20}$ between 0 and 7 GPa (293 K)

Experiment*	Pressure (GPa)	δ** (mm/s)	ΔE_Q (mm/s)	Γ† (mm/s)	χ^2
1	0.0	1.191(1)	2.205(2)	0.293(3)	0.62
2	4.0	1.163(1)	2.118(3)	0.345(4)	0.75
3	4.2	1.169(2)	2.109(3)	0.343(6)	0.49
4	6.0	1.149(2)	2.038(3)	0.378(5)	0.88
5	7.2	1.142(2)	1.979(4)	0.405(6)	0.98
6	5.1	1.154(2)	2.030(3)	0.364(6)	0.56
7	4.4	1.155(1)	2.053(3)	0.362(4)	0.80
8	4.14	1.161(1)	2.070(3)	0.342(4)	0.72
9	3.4	1.164(1)	2.103(3)	0.333(4)	0.61
10	2.4	1.170(1)	2.129(2)	0.329(4)	0.79
11	2.0	1.181(1)	2.161(2)	0.315(3)	0.69
12	1.9	1.182(1)	2.170(2)	0.319(4)	0.70
13	0.0‡	1.189(2)	2.196(3)	0.315(5)	0.68
10'§	4.4	1.158(1)	2.075(2)	0.346(4)	0.84
12'§	3.4	1.168(1)	2.099(2)	0.332(4)	0.78
	0.0‖	1.192(1)	2.208(2)	0.294(3)	

Note: Standard deviations are given in parentheses.

* Consecutively in the numbered sequence as shown in Figure 5.

** Referred to metallic Fe at ambient conditions.

† Full width at half intensity.

‡ Obtained after pressure release.

§ Experiments 10' and 12' were carried out after experiments 10 and 12, with rising pressure. These two points were not given in Figure 5.

‖ Average values by fitting relative to 13 sets of calibration data of metallic Fe taken over 3 months.

within less than 1%. No systematic asymmetry in intensity or width could be found in the high-pressure spectra. For this reason the ^{57}Fe hyperfine parameters were determined by fitting the spectra through direct solution of the Hamiltonian for the nuclear quadrupole interaction based on one experimental line width, neglecting possible effects of texture or anisotropic vibrational displacement of ^{57}Fe.

RESULTS

The ^{57}Fe spectrum of paramagnetic clinopyroxenes along the join $CaFeSi_2O_6$-$CaMgSi_2O_6$ at 293 K consists of a single doublet, which is assigned to Fe^{2+} at the octahedrally coordinated M1 sites. This holds for all the spectra between ambient pressure and 10 GPa. The doublet was well resolved over the entire range of pressures studied. The fitted parameters were background counting rate (assumed to be independent of Doppler velocity), center position, splitting, intensity, and line width of the doublet. Two typical spectra recorded at ambient pressure and 10 GPa are shown in Figure 3. The ^{57}Fe hyperfine parameters obtained from the fits are listed in Tables 1, 2, and 3.

Experimental error of the ^{57}Fe hyperfine parameters

An estimate of the total experimental error is important in view of the rather small pressure-induced changes in the hyperfine data and the relatively long recording time of a high-pressure spectrum. The statistical error of the fit was considered using χ^2 as criterion for the deviations between the counting data and the fitted Lorentzians. Determination of the total error including all systematic contributions is, however, much more involved. The following procedure has been adopted in this study. A spectrum of a metallic Fe absorber was taken before and after each high-pressure spectrum of the studied sample. The difference between the hyperfine parameters of the experimental spectrum using the two sets of calibration data should to some extent account for the experimental error resulting from the instability of the electronic system, mechanical driving device, etc. A time-dependent test of the systematic error was also undertaken by fitting a spectrum relative to a series of calibration data taken over a time span of 3 months. These results are included in Table 2 (last line). In summary, it is concluded that the total error of position and splitting of the doublet was smaller than 0.01 mm/s.

Pressure-dependent line broadening

Substantial line broadening was observed with increasing pressure. In the case of hedenbergite the widths Γ of

TABLE 3. Values of ^{57}Fe hyperfine parameters at M1 in $Hd_{60}Di_{40}$ between 0 and 8 GPa (293 K)

Pressure (GPa)	δ* (mm/s)	ΔE_Q (mm/s)	Γ** (mm/s)	χ^2
0.0	1.191(2)	2.106(4)	0.339(7)	1.37
0.9	1.181(2)	2.067(4)	0.334(9)	1.08
2.3	1.173(2)	2.050(4)	0.348(7)	1.38
3.6	1.182(2)	2.038(4)	0.351(7)	1.32
3.9	1.161(3)	1.962(7)	0.371(11)	1.16
4.6	1.162(3)	1.935(6)	0.382(9)	1.04
5.2	1.152(3)	1.910(6)	0.395(11)	1.56
5.8	1.150(3)	1.906(5)	0.406(9)	1.20
6.4	1.149(3)	1.893(5)	0.413(9)	1.45
6.7	1.149(3)	1.886(6)	0.417(10)	1.18
7.9	1.135(3)	1.827(6)	0.428(10)	1.61

Note: Standard deviations are given in parentheses. Spectra at 2.3, 3.6, 5.2, 6.4, 7.9 GPa were taken in the rising pressure experiment and 6.7, 5.8, 4.6, 3.9, 0.9, 0.0 GPa in the releasing pressure experiment.

* Referred to metallic Fe at ambient conditions.

** Full width at half intensity.

TABLE 4. Pressure and volume dependence of δ, δ_{SOD}, ΔE_Q, and Γ of hedenbergite

	Range of P (GPa)	
	0–4.2	4.4–9.9
$\partial\delta/\partial P$ (mm/s GPa)	-8×10^{-3}	-4×10^{-3}
$\partial\delta/\partial \ln V$ (mm/s)	1.03	2.23
γ	1.50	5.81
$\partial\delta_{SOD}/\partial \ln V$ (mm/s)	0.15	0.57
$\Delta\delta_{SOD}$ (mm/s)	5×10^{-4}	6×10^{-3}
$\partial\Delta E_Q/\partial P$ (mm/s GPa)	−0.029	−0.015
$\partial\Gamma/\partial P$ (mm/s GPa)	0.014	0.007

the lines increased from 0.30 mm/s at ambient pressure to 0.46 mm/s at 10 GPa (51%). For $Hd_{80}Di_{20}$ and $Hd_{60}Di_{40}$ the broadenings were 38 and 26%, respectively. The increasing line width with increasing pressure was due in part to a pressure gradient over the sample area, which produces a distribution of ΔE_Q across the sample area. The $\partial\Delta E_Q/\partial P$ values determined from Tables 1, 2, and 3 are collected in Table 4.

Pressure dependence of the center shift δ

The center shift δ, i.e., the shift of the geometrical center of the ^{57}Fe doublet, may be written as

$$\delta(T,P) = \delta_0(P) + \delta_{SOD}(T,P) \quad (1)$$

where δ_0 is the chemical or isomer shift at 0 K, $\delta_{SOD}(T,P)$ is the second-order Doppler (SOD) shift; the value of δ_{SOD} of Fe^{2+} in octahedrally coordinated sites of chain silicates at ambient conditions is about $\delta_{SOD} = -0.23$ mm/s (e.g., Lin et al., in preparation). In this study it is considered to be independent of the Fe/Mg ratio. It should be noted that δ in the present paper is referred to pyroxene at 293 K, whereas in previous studies it has been often referred to pyroxene at 78 K.

The pressure derivative of the δ at constant temperature, $(\partial\delta/\partial P)_T$, consists mainly of two contributions:

$$(\partial\delta/\partial P)_T = \partial\delta_0/\partial P + (\partial\delta_{SOD}/\partial P)_T. \quad (2)$$

By adopting the Debye model, $(\partial\delta_{SOD}/\partial P)_T$ can be estimated from the Grüneisen parameter γ and the Debye temperature θ_D (Williamson, 1978), taking into account that

$$\partial\delta_{SOD}/\partial \ln V = \gamma(9k\theta_D/16Mc)F(T/\theta_D). \quad (3)$$

In Equation 3 V is the volume of the unit cell, k is the Boltzmann constant, M is the mass of the resonant nucleus, and c is the velocity of light. The Grüneisen parameter $\gamma = \alpha V/\beta C_V$ may be obtained approximately by calculating the volume expansivity at constant pressure α, the volume compressibility at constant temperature β using the high-temperature (Cameron et al., 1973) and high-pressure (Zhang et al., 1989) data of hedenbergite, and the heat capacity at constant volume C_V, which was approximated by C_P calculated for diopside using the relationship of Krupka et al. (1985).

The F value in Equation 3 may be formulated as

$$F(T/\theta_D) = 1 + 8/(e^{\theta_D/T} - 1) - 24(T/\theta_D)^4 \times \int_0^{\theta_D/T} x^3\,dx/(e^x - 1). \quad (4)$$

In Equation 4 $x = h\nu/kT$, where h is the Planck's constant and ν is the frequency of harmonic oscillators; θ_D was taken from Kieffer (1985) for diopside.

The $(\partial\delta_{SOD}/\partial \ln V)_T$ values calculated in this way are listed in Table 4. They show that the volume dependence of δ_{SOD} is about 1 order of magnitude smaller than that of δ; δ_{SOD} should, therefore, not be neglected generally. For our simplified discussion in this paper, the pressure dependence of δ_{SOD} will be ignored. The δ_{SOD} is considered to be independent of pressure and Fe/Mg ratio of the sample, δ being interpreted in terms of δ_0.

Discontinuity of δ and ΔE_Q between 3.8 and 4.3 GPa

Generally, δ and ΔE_Q of ^{57}Fe at M1 in $Ca(Fe,Mg)Si_2O_6$ clinopyroxenes decrease with increasing pressure between ambient pressure and 10 GPa as shown in Figures 4 and 5. The reductions of δ for Hd, $Hd_{80}Di_{20}$, and $Hd_{60}Di_{40}$ are 0.08, 0.05, and 0.06 mm/s, and those of ΔE_Q are 0.36 (15.9%), 0.23 (12.7%), and 0.28 mm/s (16.5%), respectively. This study demonstrates the existence of abrupt changes between 3.8 and 4.3 GPa in δ and ΔE_Q. This is particularly pronounced for ΔE_Q, where a reduction of 0.07–0.10 mm/s (about 4%) occurs. For δ, the change between 3.8 and 4.3 GPa is small (about 0.015 mm/s at 4.3 GPa for hedenbergite). If Mg is substituted for Fe in hedenbergite the discontinuity occurs at a somewhat lower pressure. In the cases of $Hd_{80}Di_{20}$ and $Hd_{60}Di_{40}$, however, the precision of δ and ΔE_Q determination is somewhat reduced because of a nonstatistical distribution of Fe^{2+} and Mg^{2+} over the M1 sites, producing some line broadening.

Sample $Hd_{80}Di_{20}$ was studied in detail for hysteresis behavior. For this, experiments were carried out consecutively from ambient pressure to 7.2 GPa and back to ambient pressure. A hysteresis was observed between 1.9 and 7.2 GPa. An additional spectrum was taken at ambient pressure after releasing pressure (point 13 in Fig. 5) and another one after increasing pressure to 1.9 GPa (point 12 in Fig. 5) for a second time as part of the same series. This procedure yielded consistently reproducible hyperfine parameters (cf. Fig. 5). The onset of the abrupt change may be estimated to be between 4.0 and 4.2 GPa.

Compressibilities in the system $Ca(Fe,Mg)Si_2O_6$

For an interpretation of the $\partial\delta/\partial P$ and $\partial\Delta E_Q/\partial P$, information on the compression of the local volume around the position of the resonantly absorbing nucleus is needed over the pressure range studied. Unfortunately, the pressure dependence of the atomic positions between ambient pressure and 10 GPa is not well known for crystal structures of the system $Ca(Fe,Mg)Si_2O_6$. The unit-cell volumes between ambient pressure and 10 GPa were determined for Hd and $Hd_{60}Di_{40}$ by Zhang et al. (1989) from the polycrystalline samples used in this study. Single-crystal data on the compression of the M1 polyhedron in

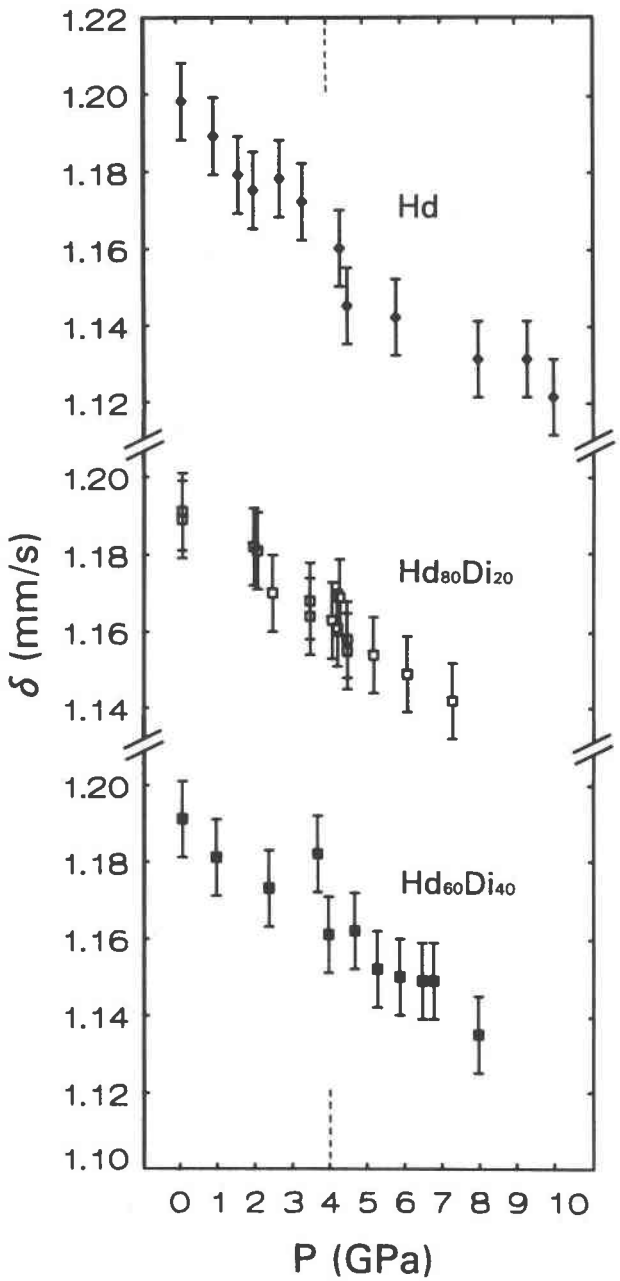

Fig. 4. Dependence of δ of hedenbergite, $Hd_{80}Di_{20}$, and $Hd_{60}Di_{40}$ on pressure. There is a discontinuity at approximately 4 GPa (cf. dashed line).

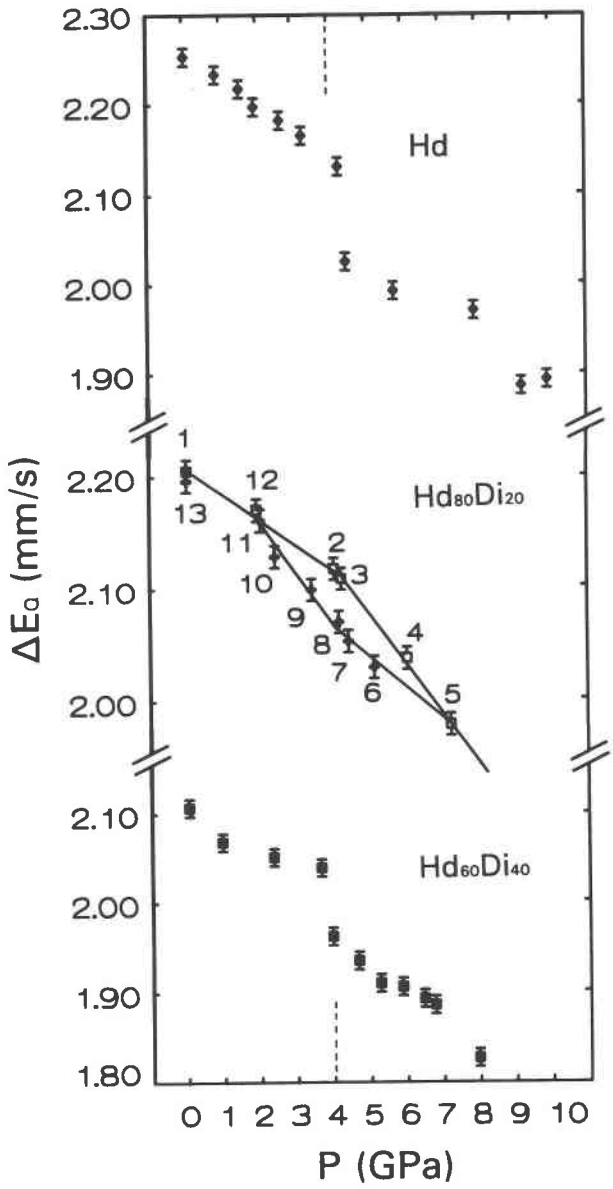

Fig. 5. Dependence of ΔE_Q of Hd, $Hd_{80}Di_{20}$, and $Hd_{60}Di_{40}$. There is a discontinuity at approximately 4 GPa (cf. dashed line). The data of $Hd_{80}Di_{20}$ were taken consecutively as listed in Table 2, where the same numbers are used. They yield a pressure hysteresis.

diopside between ambient pressure and 5 GPa were reported by Levien and Prewitt (1981).

Hedenbergite and $Hd_{60}Di_{40}$ exhibit anisotropic compression, **b** being the most compressible direction. In hedenbergite the compression along **a** is clearly smaller than along **c**, whereas in $Hd_{60}Di_{40}$ it is apparently about the same in those directions. The experimental errors of the $Hd_{60}Di_{40}$ data were, however, larger than those of hedenbergite. The compressibilities β_a, β_b, and β_c for the system $Ca(Fe,Mg)Si_2O_6$ are listed in Table 5.

The unit-cell volume of hedenbergite decreases between ambient pressure and 5 GPa by 3.3%. The bulk moduli K_0 were calculated from a least-squares fit of the pressure-volume data using a Birch-Murnaghan equation of state. For this, $(\partial K_0/\partial P)_T = 4$ was assumed. K_0 of hedenbergite is in agreement with the previous determination of Kandelin and Weidner (1988) from Brillouin spectroscopy. The K_0 values obtained for several compositions of the system $Ca(Fe,Mg)Si_2O_6$ are presented in Table 6. They do not reveal any dependence on the Fe/Mg ratio within the experimental error.

TABLE 5. Axial and volume compressibilities of clinopyroxenes $Ca(Fe,Mg)Si_2O_6$

	β_a	β_b	β_c	β_V	
	($\times 10^{-3}$/GPa)				β_a:β_b:β_c
Hd*	2.22(8)	3.3(1)	2.6(1)	7.62(7)	0.65(4):1.00(6):0.79(6)
$Hd_{60}Di_{40}$**	1.9(2)	3.1(2)	2.2(2)	6.5(2)	0.6(1):1.0(1):0.7(1)
Di†	2.58(3)	3.274(7)	2.597(3)	7.85(1)	0.78(1):1.00(4):0.793(2)

Note: β_a, β_b, β_c are the axial compressibilities, β_V is the volume compressibility; errors calculated using error propagation procedure.
* 0.0–3.7 GPa (Zhang et al., 1989).
** 0.0–4.9 GPa (Zhang et al., 1989).
† 0.0–5.3 GPa (Levien and Prewitt, 1981).

DISCUSSION

The hyperfine parameters δ and ΔE_Q are sensitive probes of the pressure-dependent electronic structure at the Fe^{2+} sites in the crystal. In the following sections the relationships between δ, ΔE_Q, compression, and Fe/Mg ratio in $Ca(Fe,Mg)Si_2O_6$ pyroxenes are discussed.

Pressure dependence of δ

The value of δ (neglecting δ_{SOD}) is proportional to the electronic charge density $\rho(0)$ at the resonantly absorbing nucleus. For ^{57}Fe, δ decreases with increasing $\rho(0)$: $\delta = \alpha\Delta\rho(0)$, where α is a nuclear constant with a negative sign for ^{57}Fe. In general (Gütlich et al., 1978), $\rho(0)$ may be considered as

$$\rho(0) = \rho_c^{\text{free ion}}(0) + \rho_{ov}(0) + \rho_{val}(0). \quad (5)$$

In the case of high-spin Fe^{2+}, $\rho_c^{\text{free ion}}(0)$ is the 1s, 2s, 3s contribution of the free Fe^{2+} core, $\rho_{ov}(0)$ is the overlap contribution $\rho_{ov}(0) = \rho_c(0) - \rho_c^{\text{free ion}}(0)$, where $\rho_c(0)$ is the contribution of the 1s, 2s, 3s orbitals of the effective Fe^{2+} core, and $\rho_{val}(0)$ is the contribution from the 3d, 4s, 4p valence orbitals of Fe^{2+} and 2s, 2p orbitals of O^{2-}. The two terms $\rho_{ov}(0)$ and $\rho_{val}(0)$ are expected to be dependent on compression. It should be noted that an effect of pressure on δ is possible only by change in bond distances and bond angles around the position of the resonantly absorbing nucleus. It is, therefore, necessary to interpret $\partial\delta/\partial P$ in terms of compression.

It is known that for pressures smaller than 5.3 GPa, the compression of the unit-cell volume V in diopside is primarily due to the compression of the M1 and M2 polyhedral volumes V_{M1} and V_{M2} (Levien and Prewitt, 1981). It is proposed that this is also valid for hedenbergite since the relative reduction in V is similar for diopside and hedenbergite in that range of pressures (Zhang et al., 1989). Consequently, $\partial\delta/\partial \ln V$ and $\partial\delta/\partial \ln V_{M1}$ in hedenbergite may be regarded as similar. Values of $\partial\delta/\partial \ln V$ for hedenbergite and $Hd_{60}Di_{40}$ calculated from data of Tables 1 and 3 and lattice parameters obtained by Zhang et al. (1989) are listed in Table 7.

Experimental high-pressure studies of ^{57}Fe resonance in FeF_2 and molecular orbital calculations of $\rho(0)$ (Reschke et al., 1977, and references cited therein) showed that $\rho_{ov}(0)$ increases with increasing pressure, whereas $\rho_{val}(0)$ decreases. The observed net decrease of δ was, therefore, ascribed to a predominant contribution of $\rho_{ov}(0)$, i.e., increased overlap between the s orbitals of the Fe^{2+} core and the valence orbitals of the ligands. The decrease of $\rho_{val}(0)$ results from a decrease of Fe^{2+} 4s population coupled with an increase of Fe^{2+} 3d population. The crystal structure of FeF_2 is of the rutile type, Fe^{2+} being octahedrally coordinated. The volume compression of the FeF_6 octahedra in FeF_2 is 4.1% between ambient pressure and 4 GPa. The electronic state of Fe^{2+} at M sites as well as the degree of covalent Fe^{2+}-ligand participation in chain silicates may be expected to be comparable to those of FeF_2.

The linear relationship between δ and V as well as the comparatively small magnitude of $\partial\delta/\partial \ln V$ in hedenbergite between ambient pressure and 4.2 GPa suggest that the observed net increase in $\rho(0)$ results mainly from the compression of the valence orbitals due to bond shortening, without changing $\rho_{ov}(0)$ significantly. At pressures >4.2 GPa, however, $\partial\delta/\partial \ln V$ is greater than in the lower range of pressures. This implies that additional fac-

TABLE 6. Bulk moduli (Mbar) of clinopyroxenes

Sample		K_0*	Reference
Hd**	synthetic	1.19(2)	this work
$Hd_{60}Di_{40}$†	synthetic	0.827(1)	this work
Hedenbergite	natural	0.71(2)	a
Hedenbergite	synthetic	1.20	b
Fassaite	natural	0.991(5)	c
Diopside	natural	1.146(4)	d
Diopside	natural	1.22(2)	e

Note: a = Vaidya et al. (1973), b = Kandelin and Weidner (1988), c = Hazen and Finger (1977), d = Levien and Prewitt (1981), e = McCormick et al. (1989).
* Fitted by use of a Birch-Murnaghan equation of state assuming $K_0' = 4.0$.
** Fitted to data ≤ 3.7 GPa.
† Fitted to data ≤ 3.1 GPa.

TABLE 7. Volume coefficients of δ and ΔE_Q

Sample	Pressure range (GPa)	$(\partial\delta/\partial \ln V)$	$(\partial\Delta E_Q/\partial \ln V)$
Hd	0.0–4.2	1.03	3.67
	4.4–9.9	2.23	7.19
$Hd_{60}Di_{40}$	0.0–3.6	0.67	1.54
	3.9–7.9	0.96	3.82

Note: V calculated from the lattice constants of Zhang et al. (1989).

tors are important. The increase of $\partial\delta/\partial \ln V$ at pressures >4.2 GPa cannot be attributed to a concomitantly higher compressibility, since the compressibility decreases at higher pressure. There must be excess change in $\rho_{ov}(0)$ that additionally contributes to $\rho(0)$ at pressures >4.2 GPa. This is just what was found in FeF_2 (Reschke et al., 1977).

The pressure dependence of δ at the M1 site in hedenbergite may also be compared with that of metallic Fe. The $\partial\delta/\partial P$ coefficient of α Fe (ground state $3d^6 4s^2$) is -7.46 to -9.08×10^{-3} mm/s GPa. The value $\partial\delta/\partial P = -8 \times 10^{-3}$ mm/s GPa (Table 4) for hedenbergite between ambient pressure and 4.2 GPa is similar to that of α Fe. Williamson (1978) pointed out that the $\partial\delta/\partial P$ in metallic and ionic compounds are generally comparable. The decrease in δ for α Fe was interpreted by Williamson (1978) mainly in terms of compression of the 4s orbital.

Pressure dependence of ΔE_Q

The ^{57}Fe quadrupole splitting ΔE_Q is determined by the maximum value V_{ZZ} of the second derivative V_{ii} ($i = X, Y, Z$) and the asymmetry parameter $\eta = (V_{XX} - V_{YY})/V_{ZZ}$. Here V is the electrostatic potential at the nuclear site. The contribution of η to ΔE_Q is minor (maximum 15% for $\eta = 1$). The value of η for M1 in hedenbergite at 4.2 K is small (Coey and Ghose, 1985). At temperatures near 293 K, however, η is large (Stanek et al., 1986b). At any rate, the contribution of the change in η to ΔE_Q is neglected here.

In the case of high-spin Fe^{2+} in predominantly ionic compounds, V_{ZZ} can be separated into three additive terms (Gütlich et al., 1978): (1) the valence contribution V_{ZZ}^{val}, which results from the unbalanced population of 3d orbitals, (2) the lattice contribution V_{ZZ}^{lat}, which originates from the noncubic distribution of ligand charges and the more distant ions around the Fe^{2+} site, and (3) V_{ZZ}^{ov}, which accounts for the overlap between Fe^{2+} and ligand orbitals. It is often difficult to arrive at conclusions from variation of ΔE_Q alone about the individual changes in these three components of V_{ZZ}. In principle V_{ZZ}^{val} provides the predominant contribution to V_{ZZ} and determines the sign. V_{ZZ}^{lat} is minor and of opposite sign. The sign of V_{ZZ}^{ov} is also opposite to that of V_{ZZ}^{val}.

If it is assumed that the M1 octahedra in hedenbergite remain geometrically similar with increasing pressure, V_{ZZ}^{lat} is expected to increase simply because of bond shortening due to compression. This increase from ambient pressure to 5.3 GPa is calculated to be about 5% for the M1 octahedron using the data for diopside of Levien and Prewitt (1981).

The effect of deviation of the M1 octahedron from cubic symmetry on ΔE_Q may be estimated considering crystal-field splitting (Ingalls, 1964). For the case of quasi-axial symmetry ($\eta = 0$), ΔE_Q can be expressed in terms of a reduction function F as

$$\Delta E_Q = C\alpha^2 F(\Delta, \alpha^2\lambda_0, T). \quad (6)$$

In Equation 6 C is a constant, Δ is the energy separation between the $3d_{XY,XZ,YZ}$ energy levels of Fe^{2+}, α^2 is the isotropic covalency factor, λ_0 is the spin orbit coupling constant of the free Fe^{2+} ion, and T is the temperature.

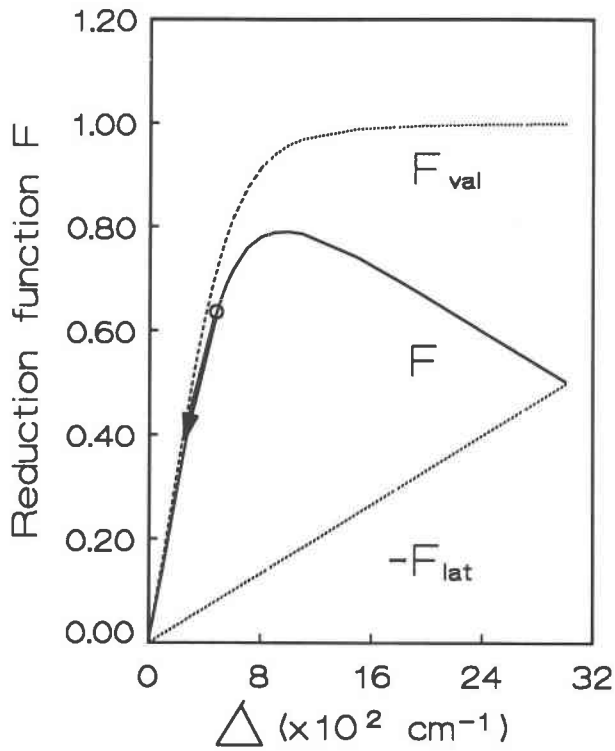

Fig. 6. Reduction function F depending on pseudoaxial crystal-field splitting Δ of $3d_{XY,XZ,YZ}$. F^{val} is the contribution due to V_{ZZ}^{val}, F^{lat} that due to V_{ZZ}^{lat}; Δ, derived from ^{57}Fe ΔE_Q measurements of hedenbergite between 7 and 293 K, is marked as open circle. The arrow designates the change in F with increasing pressure.

First, the behavior of ΔE_Q at pressures below 4.2 GPa is considered. A study of the temperature dependence of ΔE_Q (Lin et al., in preparation) at M1 in orthopyroxene between 7 and 293 K yielded $\Delta = 480$ cm^{-1} and $\alpha^2 = 0.72$, assuming an effective axial crystal field. Using the same procedure, $\Delta = 515$ cm^{-1} and $\alpha^2 = 0.61$ was obtained for M1 in hedenbergite (Zhang, unpublished data). From the characteristics of F it is clear that for hedenbergite an increase of Δ is associated with an increase of F. This is shown in Figure 6. The increase of Δ should be interpreted as an increase of the pseudoaxial distortion. The observed decrease of ΔE_Q with increasing pressure implies, therefore, that the pseudoaxial distortion of M1 becomes smaller. Similar observations on the relationship between polyhedral distortion at the Fe^{2+} position and pressure have also been made for FeF_2 (Champion et al., 1967; Drickamer et al., 1969). Comparable crystallographic results were reported for a fassaitic clinopyroxene, where it was found that the compressibility of the shortest bond in the M1 octahedron is small and that of the longest bond is large (Hazen and Finger, 1977). On the other hand, Levien and Prewitt (1981) apparently

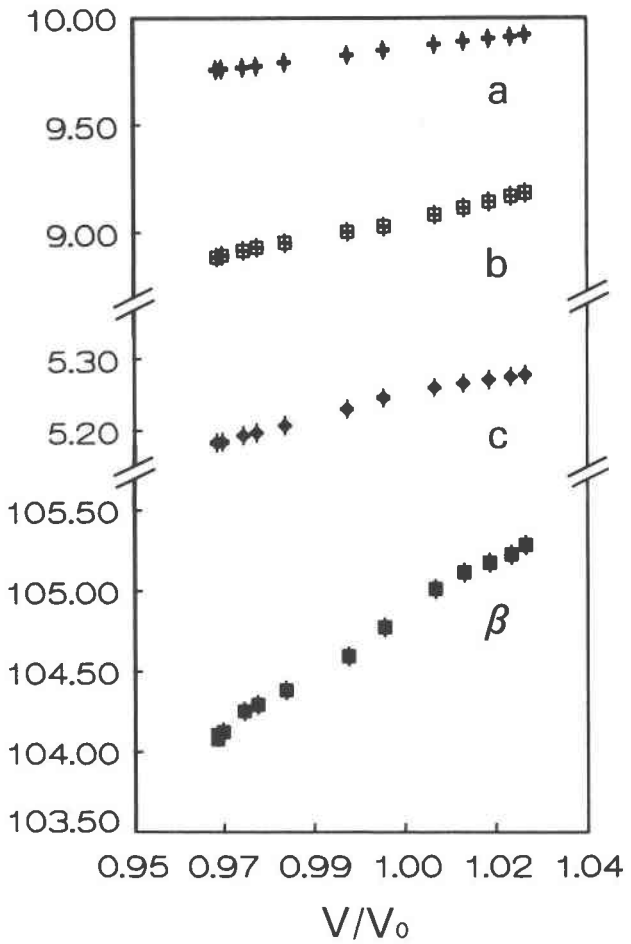

Fig. 7. Unit-cell parameters of hedenbergite at high pressures and high temperatures vs. volume ratio V/V_0. The data show inverse behavior of unit-cell parameters at high temperatures and pressures. Units of the ordinate are in ångströms for *a*, *b*, and *c* and in degrees for β.

found no change in the polyhedral geometry of the M1 in diopside up to 5.3 GPa.

It is not clear yet which factors contribute to V_{zz} at pressures higher than 4.2 GPa, where the overlap of the orbitals between Fe and O is greater. Similar to the behavior of $\partial\delta/\partial \ln V$, $\partial\Delta E_Q/\partial \ln V$ is substantially higher above 4.2 GPa compared with that at lower pressures (Table 7). This may be accounted for by enhanced covalent participation coupled with distinct polyhedral distortion at pressures above 4.2 GPa.

Inverse effect of *P* and *T* on the unit-cell parameters

The comparison of the high-pressure data of Zhang et al. (1989) with the high-temperature data of Cameron et al. (1973) shows an inverse relationship of the effects of pressure and temperature on all unit-cell parameters of hedenbergite. This is illustrated in Figure 7. Levien and Prewitt (1981) also showed this to be the case for diopside. An inverse relationship also exists for the ratios a/b and b/c (Fig. 8); $[\partial(a/c)/\partial T]_P$ and $[\partial(a/c)/\partial P]_T$ are both positive. The consequence of this is $\beta_c > \beta_a$, whereas $\alpha_c < \alpha_a$.

Effect of chemical composition at constant pressure

There are two important conclusions from the data of Tables 1, 2, and 3. First, if the δ and ΔE_Q values are plotted against each other as shown in Figure 9, an approximately linear increase of ΔE_Q with increasing δ is observed for each of the three chemical compositions studied. Second, δ plotted against the Fe/Mg ratio at constant pressure is nearly invariable, whereas ΔE_Q systematically decreases with decreasing Fe/Mg ratio. This implies that there is no dependence between δ and ΔE_Q for the three chemically different samples at any constant pressure. This is also in agreement with the results of Dollase and Gustafson (1982) at ambient pressure.

It is known that the bond distances of the M1 polyhedra in $Ca(Fe,Mg)Si_2O_6$ clinopyroxenes decrease with increasing pressure at constant Fe/Mg ratio; they also decrease with decreasing Fe/Mg ratio at ambient pressure. For example, the shortest bond is $d_{Fe\text{-}O} = 2.087$ Å and the average bond is $\langle d\rangle_{Fe\text{-}O} = 2.130$ Å at M1 in hedenbergite, and $d_{Mg\text{-}O} = 2.050$ Å and $\langle d\rangle_{Mg\text{-}O} = 2.077$ Å at M1 in diopside at ambient conditions (Cameron et al., 1973). The relative reduction of 2.5% of $\langle d\rangle$ from hedenbergite to diopside at ambient pressure corresponds to a reduction of 1.7% in diopside from ambient pressure to 5 GPa (Levien and Prewitt, 1981). In view of the pronounced reduction of δ at high pressure (0.04 mm/s at 4 GPa, cf. Table 1), the invariance of δ to the substitution of Mg for Fe at constant pressure is remarkable. It implies relatively invariable Fe-O bonds at M1 sites occupied by Fe compared with the corresponding average (Fe,Mg)-O bonds at all M1 sites, at least in the Fe-rich part of the $Ca(Fe,Mg)Si_2O_6$ system. In view of the definition of δ in terms of $\rho(0)$, especially the shortest Fe-O bond of the FeO_6(M1) octahedron seems to be invariable.

The decrease of ΔE_Q with increasing Mg^{2+} substitution is mainly the result of the change in V_{ZZ}^{val}, according to Figure 6. It is indicative of a decrease of the pseudoaxial crystal-field splitting Δ of Fe^{2+} with increasing Mg substitution at M1. The change in the splitting of the $3d_{XY,XZ,YZ}$ levels practically does not change the relative s, d electron densities as concluded from the invariance of δ. This is different at high pressures, where both s and d electron densities change with increasing pressure.

Phase transition

It is well established that γ resonance may be sensitive to phase transitions since hyperfine parameters such as δ and ΔE_Q are implicit expressions of the electronic configuration and lattice dynamical effects (Johnson, 1989; Pipkorn et al., 1964; Petrich, 1969). From their electronic nature, δ and ΔE_Q depend also implicitly on volume and entropy. They provide, therefore, information on the nature of a phase transition (Preston, 1978).

The abrupt discontinuities in δ and ΔE_Q found between

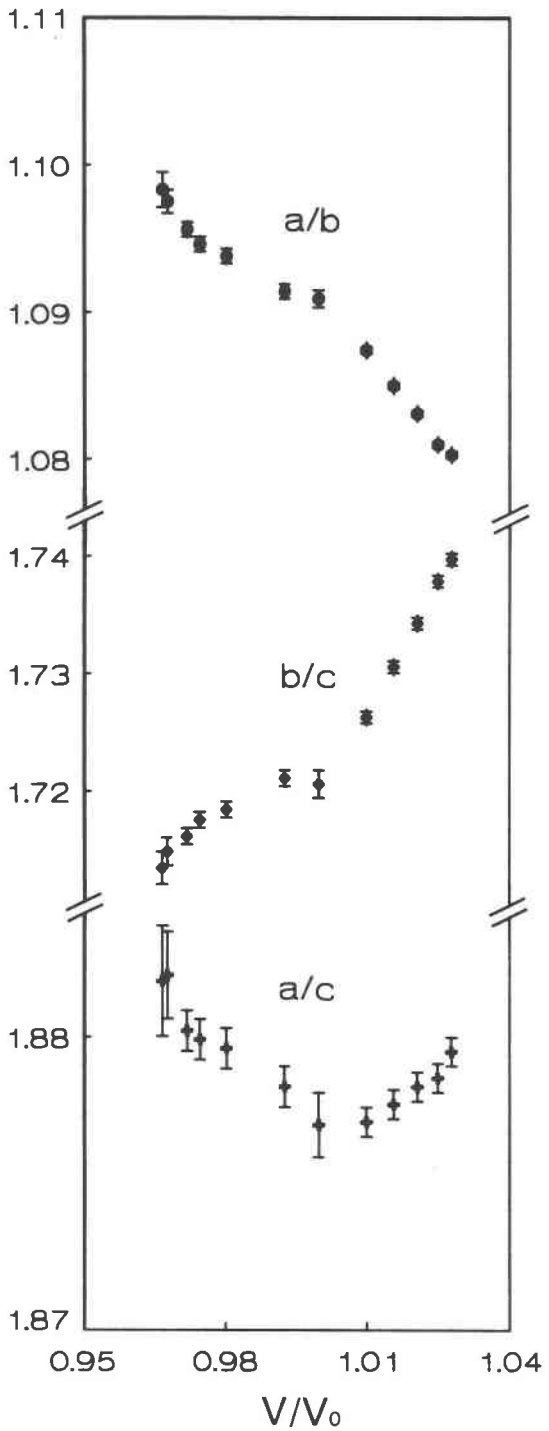

Fig. 8. Axial ratios a/b, b/c, and a/c vs. V/V_0.

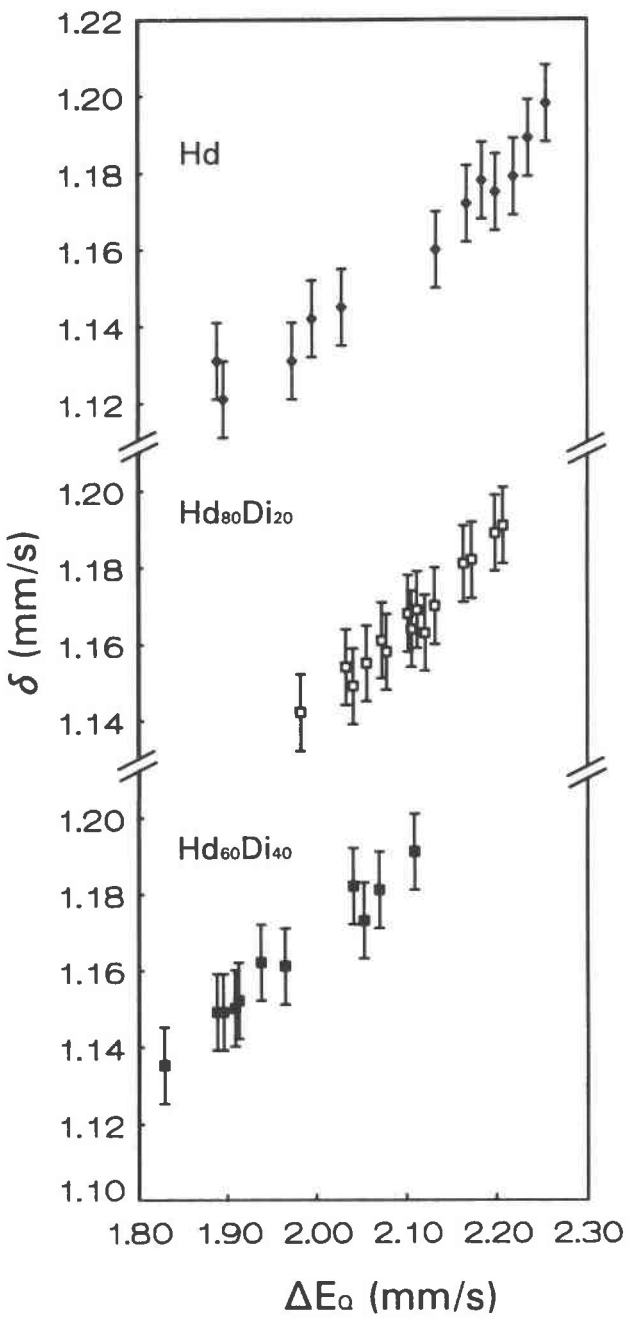

Fig. 9. Approximate linear relationships between δ and ΔE_Q at high pressures in Hd, $Hd_{80}Di_{20}$, and $Hd_{60}Di_{40}$.

3.8 and 4.3 GPa are characteristic of a first-order phase transition. The more pronounced discontinuity in ΔE_Q than in δ indicates that changes in electronic structure due to octahedral distortion play a more important role than simple compression.

The hysteresis in ΔE_Q found in $Hd_{80}Di_{20}$ provides additional evidence that the phase transition is thermodynamically of first order. Two coexisting phases, however, could not be resolved in the spectra, probably because of the rather small structural changes, the line broadening due to a pressure gradient over the absorber area, or both. The phase transition is reversible. It could be of the displacive type. Prewitt et al. (1971) reported a thermal hysteresis for the $P2_1/c$-$C2/c$ transition observed in natural pigeonite. This was revealed recently to be a first-order

phase transition by transmission electron microscopy at elevated temperatures (Shimobayashi and Kitamura, 1990).

Examination of high-pressure powder X-ray diffraction data on the same samples showed changes in the pressure derivatives of the cell parameters and small discontinuities at 4 GPa, especially for the c axis (Zhang et al., 1989), the angle β, and the volume. The volume-pressure data over the entire range of pressures studied, however, cannot be fitted reasonably using a Birch-Murnaghan equation of state. More diffraction data at pressures higher than 5 GPa are needed for further clarification.

Conclusions

Fe at M1 in clinopyroxenes $Ca(Fe,Mg)Si_2O_6$ is in the high-spin ferrous state between ambient pressure and 10 GPa. Changes in isomer shift δ and quadrupole splitting ΔE_Q reflect primarily changes in Fe^{2+} electronic structure, whereas lattice dynamical effects such as SOD and change in recoil-free fraction at high pressures are found to be small.

The value of δ decreases with increasing pressure because of a compression of the valence shell of Fe^{2+}. At pressures higher than 4 GPa, additional contributions to δ are due to overlap between s orbitals of Fe^{2+} and valence orbitals of the ligands. The value of ΔE_Q decreases with increasing pressure mainly because of a change in the distribution of the $3d^6$ electron over the $d_{XY,XZ,YZ}$ levels related to a change in pseudoaxial distortion. The effect of simple lattice compression on ΔE_Q is small. At pressures higher than 4 GPa, the effects of increased covalent participation in the Fe^{2+}-ligand bonds and octahedral distortion on ΔE_Q are relatively enhanced.

Substitution of Mg^{2+} for Fe^{2+} at M1 in the Fe-rich part of the system changes the geometrical configuration of the Fe^{2+} octahedra, the shortest Fe-O bonds, however, remaining nearly invariable. This is indicative of distinct Fe-O and Mg-O bonds at the crystallographically equivalent M1 positions.

The unit cell of hedenbergite shows anisotropic compression: $\beta_b > \beta_c > \beta_a$. An inverse behavior of all unit-cell parameters with increasing pressure and increasing temperature is observed.

Discontinuities in the pressure dependence of δ and ΔE_Q between 3.8 and 4.3 GPa indicate a reversible phase transition of first order.

Acknowledgment

We thank G. Steinbach for technical assistance; J. Moser, Physics Department, Technical University of Munich, for advice about the high-pressure experiments; Chuanyi Lin, Guangzhou Branch, Institute of Geochemistry, Academia Sinica, for his help in the calculation of crystal-field splitting; and David Virgo, Carnegie Institution of Washington, for his constructive review. This work was financially supported by Deutsche Forschungsgemeinschaft and Bundesministerium für Forschung und Technologie grant HA1MAR6.

References cited

Burns, R.G., Tossell, J.A., and Vaughan, D.J. (1972) Pressure-induced reduction of a ferric amphibole. Nature, 240, 33–35.

Cameron, M., Sueno, S., Prewitt, C.T., and Papike, J.J. (1973) High-temperature crystal chemistry of acmite, diopside, hedenbergite, jadeite, spodumene, and ureyite. American Mineralogist, 58, 594–618.

Champion, A.R., Vaughan, R.W., and Drickamer, H.G. (1967) Effect of pressure on the Mössbauer resonance in ionic compounds of iron. Journal of Chemical Physics, 47, 2583–2590.

Coey, J.M.D., and Ghose, S. (1985) Magnetic order in hedenbergite: $CaFeSi_2O_6$. Solid State Communications, 53, 143–145.

Dollase, W.A., and Gustafson, W.I. (1982) ^{57}Fe Mössbauer spectral analysis of sodic clinopyroxenes. American Mineralogist, 67, 311–327.

Drickamer, H.G., Fung, S.C., and Lewis, G.K. (1969) High pressure Mössbauer studies. In R.S. Bradley, Ed., Advances in high pressure research, vol. 3, p. 1–40. Academic Press, London.

Eiling, A., and Schilling, J.S. (1981) Pressure and temperature dependence of electrical resistivity of Pb and Sn from 1–300 K and 0–10 GPa—use as continuous resistive pressure monitor accurate over wide temperature range; superconductivity under pressure in Pb, Sn, and In. Journal of Physics, F, 11, 623–639.

Gütlich, P., Link, R., and Trautwein, A. (1978) Mössbauer spectroscopy and transition metal chemistry, p. 56–83. Springer-Verlag, Berlin.

Hazen, R.M., and Finger, L.W. (1977) Compressibility and crystal structure of Angra dos Reis fassaite to 52 kbar. Carnegie Institution of Washington Year Book, 76, 512–515.

Huggins, E., Mao, H.K., and Virgo, D. (1974) Mössbauer studies at high pressure using the diamond-anvil cell. Carnegie Institution of Washington Year Book, 74, 405–410.

Ingalls, R. (1964) Electric-field gradient tensor in ferrous compounds. Physical Review, 133, A787–A795.

Johnson, C.E. (1989) The Mössbauer effect and magnetic phase transitions. Hyperfine Interactions, 49, 19–42.

Kandelin, J., and Weidner, D.J. (1988) Elastic properties of hedenbergite. Journal of Geophysical Research, 93, 1063–1072.

Kieffer, S.W. (1985) Heat capacity and entropy: Systematic relations to lattice vibrations. In Mineralogical Society of America Reviews in Mineralogy, 14, 114.

Kim, Y.H., Ming, L.C., and Manghnani, M.H. (1989) A study of phase transformation in hedenbergite to 40 GPa at 1200 °C. Physics and Chemistry of Minerals, 16, 757–762.

Krupka, K.M., Hemingway, B.S., Robie, R.A., and Kerrick, D.M. (1985) High-temperature heat capacities and derived thermodynamical properties of anthophyllite, diopside, dolomite, enstatite, bronzite, talc, tremolite, and wollastonite. American Mineralogist, 70, 261–271.

Levien, L., and Prewitt, C.T. (1981) High-pressure structure study of diopside. American Mineralogist, 66, 315–323.

Levien, L., Weidner, D.J., and Prewitt, C.T. (1979) Elasticity of diopside. Physics and Chemistry of Minerals, 4, 105–113.

McCormick, T.C., Hazen, R.M., and Angel, R.J. (1989) Compressibility of omphacite to 60 kbar: Role of vacancies. American Mineralogist, 74, 1287–1292.

Moser, J., Gal, J., Potzel, W., Wortmann, G., Kalvius, G.M., Dunlap, B.D., Lam, D.J., and Spirlet, J.C. (1980) High pressure Mössbauer studies of magnetic Np intermetallics. Physica, 102B, 199–205.

Petrich, G. (1969) Studies of magnetic phase of erbium compounds. Zeitschrift für Physik, 221, 431–450 (in German).

Pipkorn, D.N., Edge, C.K., Debrunner, P., Pasquali, G.De., Drickamer, H.G., and Frauenfelder, H. (1964) Mössbauer effect in iron under very high pressure. Physical Review, 135, A1604–A1612.

Preston, R.S. (1978) Isomer shift at phase transitions. In G.K. Shenoy and F.E. Wagner, Eds., Mössbauer isomer shifts, p. 281–316. North-Holland, Amsterdam.

Prewitt, C.T., Brown, G.E., and Papike, J.J. (1971) Apollo 12 clinopyroxenes: High temperature X-ray diffraction studies. Proceedings of the Second Lunar Science Conference, 1, 59–68.

Reschke, R., Trautwein, A., and Harris, F.E. (1977) Electronic structure, pressure- and temperature-dependent charge densities, and electric field gradients in FeF_2. Physical Review B, 15, 2708–2717.

Shimobayashi, N., and Kitamura, M. (1990) Thermoelastic martensitic transformation between high-low clinopyroxenes. Abstracts of 15th IMA meeting, 1, 449–450.

Spijkerman, J.J., Ruegg, F.C., and de Voe, J.R. (1965) Standardization of the differential chemical shift for Fe^{57}. In I.J. Gruverman, Ed., Mössbauer effect methodology, vol. 1, p. 119. Plenum Press, New York.

Stanek, J., Hafner, S.S., and Sawicki, J.A. (1986a) Local states of Fe^{2+} and Mg^{2+} in magnesium-rich olivines. American Mineralogist, 71, 127–135.

Stanek, J., Hafner, S.S., Regnard, J.R., and El Goresy, A. (1986b) Temperature-dependent hyperfine parameters in $CaFeSi_2O_6$. Hyperfine Interactions, 28, 829–832.

Tamai, H., and Yagi, T. (1989) High-pressure and high-temperature phase relations in $CaSiO_3$ and $CaMgSi_2O_6$ and elasticity of perovskite-type $CaSiO_3$. Physics of the Earth and Planetary Interiors, 54, 370–377.

Vaidya, S.N., Bailey, S., Pasternack, T., and Kennedy, G.C. (1973) Compressibility of fifteen minerals to 45 kilobars. Journal of Geophysical Research, 78, 6893–6898.

Williamson, D.L. (1978) Influence of pressure on isomer shifts. In G.K. Shenoy and F.E. Wagner, Eds., Mössbauer isomer shifts, p. 317–360. North-Holland, Amsterdam.

Zhang, L., Ahsbahs, H., Turk, P.-G., and Hafner, S.S. (1989) A pressure induced phase transition in pyroxene. High Pressure Research, 5, 732–734.

Manuscript received February 19, 1991
Manuscript accepted December 3, 1991